Available online at www.sciencedirect.com

jmr&t Journal of Materials Research and Technology

www.jmrt.com.br

Original Article

Effects of layered double hydroxides incorporation on carbonation resistance of cementitious materials

Juntao Ma[a,d], *Ping Duan*[b,c,d,*], *Daming Ren*[b,c], *Wei Zhou*[b,c]

[a] *School of Civil Engineering and Communication, North China University of Water Resources and Electric Power, Zhengzhou 450045, P.R. China*

[b] *Faculty of Materials Science and Chemistry, China University of Geosciences, Wuhan 430074, China*

[c] *Engineering Research Center of Nano-Geomaterials of Ministry of Education, China University of Geosciences, Wuhan 430074, China*

[d] *State Key Laboratory of Silicate Materials for Architectures, Wuhan University of Technology, Wuhan 430070, China*

ARTICLE INFO

Article history:
Received 11 February 2017
Accepted 20 August 2017
Available online 24 March 2018

Keywords:
Layered double hydroxides (LDHs)
Carbonation
Anion exchange
Adsorption
Cementitious materials

ABSTRACT

The development of new or modified cementitious materials is an important part of existing strategies to improve performance and minimize life-cycle costs and to eliminate the CO_2's impact on durability. The high anion exchange capacity of layered double hydroxides (LDHs) materials makes their interlayer ion exchange by organic and inorganic anions versatile and easily achieved. LDH-like materials could be used in cementitious materials for their CO_3^{2-} capturing capacity and to enhance carbonation resistance of cementitious materials.

In this work, original LDHs were synthesized, LDHs calcined at 500, 550 and 600 °C, respectively, were prepared. Power X-ray diffraction (XRD), IR-spectroscopy and thermal analysis (TG–DSC) were employed to characterize the component and structural changes of these types of LDHs before and after CO_2 capture. Carbonation resistance of cement paste incorporating LDHs was experimentally evaluated for assessment of CO_2 capture capacity of LDHs. Ion exchange mechanism of LDHs was also analyzed from adsorption experiments.

The results show that LDH-like materials could be used for their CO_3^{2-} capturing capacity to enhance carbonation resistance of concrete as well as to eliminate CO_2's impact on durability aspect especially the LDHs calcined at 600 °C. Calcined LDHs fulfill the structure regeneration after CO_2 capture. LDHs have positive effect on improvement of carbonation resistance of cement paste especially at later curing stages.

* *Corresponding author.*
E-mails: majuntao@ncwu.edu.cn (J. Ma), dp19851128@sina.com, duanping@cug.edu.cn (P. Duan).

https://doi.org/10.1016/j.jmrt.2017.08.014

1. Introduction

In urban and industrial areas, where environmental pollution results in a significant concentration of CO_2, carbonation-initiated reinforcement corrosion prevails. Recognition of the role of anthropogenic carbon dioxide's impact on climate change in recent years has led to the need for worldwide commitments in reducing carbon dioxide (CO_2) and other greenhouse gases.

Therefore, research is currently conducted at various institutions to develop new and improved construction materials, rehabilitation and repair technologies, and a better understanding of the physical and chemical mechanisms that lead to deterioration. The improved knowledge will enable designers not only to properly rehabilitate and maintain the current stock of concrete structures, but also to improve the durability of future structures by giving, in the design stage, proper consideration to the environment and conditions. And the most important strategy is how to control the carbonation process, therefore, establishing and developing new technology for inhibiting carbonization reaction of concrete materials is the guarantee of good durability of modern concrete contains large amounts of mineral admixtures.

Hydrotalcite-like compounds (HTLCs) are a class of layered compounds that are receiving attention both as technical materials and as geologically significant phases that influence the cycling of aqueous species in the environment.

Among the group of minerals referred to as hydrotalcite-like compounds [1], the 'layered double hydroxides' (LDHs) have many physical and chemical properties that are surprisingly similar to those of clay minerals. Their layered structure, wide chemical compositions (due to variable isomorphous substitution of metallic cations), variable layer charge density, ion-exchange properties, reactive interlayer space, swelling in water, and rheological and colloidal properties make LDHs clay-like. But because of their anion-exchange properties, LDHs were referred to as 'anionic clays'. Naturally occurring hydrotalcite, $Mg_6Al_2(OH)_{16}CO_3{\cdot}4H_2O$, and synthetic hydrotalcite-like compounds, also called layered double hydroxides (LDHs), have been investigated for many years [2,3]. Taylor [4] described these phases as being structurally related to brucite the same way the AFm phases are to Portlandite. The formula of the LDHs can be generalized to $[M^{2+}{}_{1-x}M^{3+}{}_x(OH)_2]^{x+}[A^{n-}{}_{x/n}{\cdot}mH_2O]^{x-}$, where "x" represents the mole fraction (based on 1 mol of cations) in the brucite layer, M^{2+}can be Mg^{2+}, Zn^{2+}, Mn^{2+}, Ca^{2+}, etc.; M^{3+}: Al^{3+},Ga^{3+}, Fe^{3+}, Cr^{3+}, etc.; and A^{n-}: NO_3^-, Cl^-, CO_3^{2-},SO_4^{2-}, etc. [5].

The structure of an LDH is basically built up from the parent structure brucite $Mg(OH)_2$ by isomorphous substitution of divalent cations (shown in Fig. 1). The replacement of Mg^{2+} by M^{3+} ions generates an excess of positive charge within the inorganic layers, which has to be balanced by incorporation in the interlayer space of anions, such as NO_3^-, Cl^-, CO_3^{2-}, SO_4^{2-}, etc. In addition to anions, the interlayer space region can also contain water molecules connected to the inorganic layers via hydrogen bonding.

The high anion exchange capacity of LDH-like materials makes their interlayer ion exchange by organic and inorganic anions versatile and easily achieved [6–8]. LDHs have been studied extensively for a wide range of applications utilizing catalysts [9,10], ceramic precursors [11] adsorbents [12], and bio-organic nanohybrids [13,14]. Recent research has shown great flexibility of the LDH-like materials in tailoring the chemical and physical properties of materials to be used for specific applications, e.g., molecular recognition, optical storage, batteries, etc. [15,16].

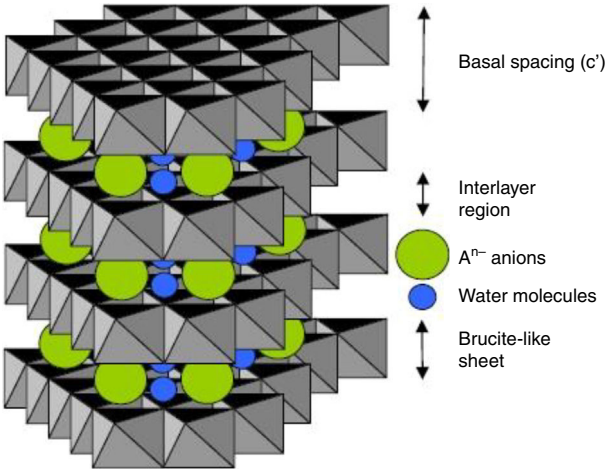

Fig. 1 – Schematic diagram of LDHs structure.

LDH solid solutions are common secondary phases in the contact zone between clays and cementitious materials. In addition to the direct synthesis by coprecipitation from salt precursors, LDHs have been subject of many post-synthesis transformations involving their well-known memory effect property and ion-exchange capacity.

These hydroxides exhibit a selectivity for the anions in the sequence $CO_3^{2-} > SO_4^{2-} > HPO_4^{2-} > F^- > Cl^- > B(OH)^{4-} > NO_3^-$, therefore, LDH-like compounds can be used as host materials for a variety of anions of interest to cement scientists. LDH-like materials could be used in cement and concrete for their CO_3^{2-} capturing capacity and to enhance carbonation resistance of concrete.

In this study, we examined the effects of LDHs containing Mg and Al on carbonation resistance of cementitious materials. Power X-ray diffraction (XRD), IR-spectroscopy and thermal analysis (TG–DSC) were employed to characterize the component and structural changes of these types of LDHs before and after CO_2 capture. Carbonation resistance of cement paste incorporating LDHs was experimental evaluated for assessment of CO_2 capture capacity of LDHs. Ion exchange mechanism of LDHs was also analyzed from adsorption experiments and structure evolution.

2. Experimental

2.1. Materials

Portland cement (CEM I 42.5) (relative density 3100 kg/m^3, specific surface area 369.6 m^2/kg) was used as binder in the study. Fly ash was used as mineral admixture. Their chemical compositions are shown in Table 1. Cement paste samples were prepared for carbonation test and micro-analysis. The replace

Table 1 – Chemical composition of Portland cement and fly ash (wt%).

	SiO_2	Fe_2O_3	Al_2O_3	CaO	MgO	SO_3	LOI	Sum
Cement	21.35	3.31	4.67	62.60	3.08	2.25	0.95	98.21
Fly ash	49.67	4.20	35.13	3.09	0.82	0.57	1.97	95.45

Table 2 – Chemical composition of LDHs (mass%).

	SiO_2	Al_2O_3	Fe_2O_3	CaO	MgO	Na_2O	SO_3	K_2O	LOI
Original LDHs	0.02	20.75	–	0.06	34.27	1.8	1.77	–	41.02
Calcinated LDHs	0.09	34.72	–	0.12	55.07	2.64	3.02	–	4.17

level of cement by fly ash was 30% at a constant water/binder (w/b) ratio of 0.4.

Samples prepared for this study were synthesized using a "memory-effect"-based synthesis route. That is, by recovering of the layered structure through calcination of the starting hydrotalcite and subsequent contact of the derived mixed oxide with solutions containing many different anions, or by direct exchange of the anions located in the interlayer space by others, an impressive variety of hydrotalcite-derived compounds have been synthesized.

Mg–Al–CO_3 hydrotalcites was synthesized using a conventional coprecipitation method. A salt solution (200 mL) containing appropriate ratios of $MgCl_2{\cdot}6H_2O$ (1.2 mol/L) and $AlCl_3{\cdot}6H_2O$ (0.4 mol/L) was created. Solution (200 mL) containing NaOH and Na_2CO_3, at sufficient concentrations were also created to precipitate the salt in the first solution. The two solutions were simultaneously added drop by drop into a 200 mL sample of deionized water, which were vigorously stirred. The temperature was fixed at 313 K, and the pH was maintained at 10–11. The resulting slurry was allowed to rest at 338 K for 12 h. The final precipitate was centrifuged several times with deionized water, until the superstratum water was free of Cl^-. The precipitate was then dried at 378 K for 8 h to obtain the Mg–Al–CO_3 type hydrotalcite powder.

Hydrotalcite-like compounds Mg–Al–CO_3 type hydrotalcite were first synthesized experimentally and then calcined at 500, 550 and 600 °C, respectively, for 4 h with a heating rate of 3 °C/min from ambient temperature, and cooled naturally to ambient temperature. Chemical composition of LDHs is measured and listed in Table 2.

Calcinations of original LDHs lead to dehydration and decarbonization, hence there exist chemical composition differences between original LDHs and calcined LDHs, especially the high content of Al_2O_3 and MgO in calcined LDHs.

2.2. *Casting and curing*

Content of LDHs was kept at constant 2% by weight of binder including cement and fly ash. The mixing sequence employed consists of dry mixing of binders including cement, fly ash and LDHs for 30 s. After ensuring proper mixing of all the solid components, polycarboxylates superplasticizer was added into water and the addition of liquids including water and superplasticizer into the dry solids was completed during 30 s. Finally, the mixing between the liquids and solids was continued for further 3 min.

Specimens with the dimensions of 40 mm × 40 mm × 40 mm were mixed and then cast in molds for various tests. The specimen surfaces were covered with polyethylene sheets to prevent loss of moisture. After 24 h, all specimens were demolded and cured at the temperature of 20 ± 2 °C and the relative humidity of 95% until the testing days.

2.3. *Characterization*

The powder X-ray diffraction (XRD) was performed on a D8 Advance X-Ray diffractometer at 45 kV and 35 mA with a graphite secondary monochromator to characterize the precipitated solids. The diagrams were recorded with Cu Kα radiation at ambient temperature within a 2θ-range from 5° to 75°, using a step size of 0.02°/s.

The compositions of the hydrotalcites bearing anions samples were analyzed using an inductively coupled plasma-mass spectrometer (ICP/MS) for the Mg and Al content, and the anion content was determined using a ion chromatograph. The content of interlayer water in these solid samples was determined by a Seiko simultaneous thermal analyzer (STA) TG/DSC in flowing Ultra zero air (150 mL/min) from room temperature to 1000 °C with a heating rate of 20 °C/min.

3. Results and discussion

3.1. *XRD patterns analyses of hydrotalcite-like compounds*

As shown in Fig. 2, the transformation of the crystalline LDH phase (O-LDHs) to nearly amorphous mixed oxide (C-LDHs) was characterized by XRD. In the XRD patterns of LDHs (shown in Fig. 2), the basal reflections from (003), (006), etc., planes and the reflection from the (110) plane are indicative of the formation of a Mg–Al–CO_3 LDH material [2]. All the solids including original LDHs, and LDHs calcined at 500, 550 and 600 °C, respectively, after CO_2 capture (hereafter were referred to as C-O-LDHs, C-500C-LDOs, C-550C-LDOs and C-600C-LDOs,

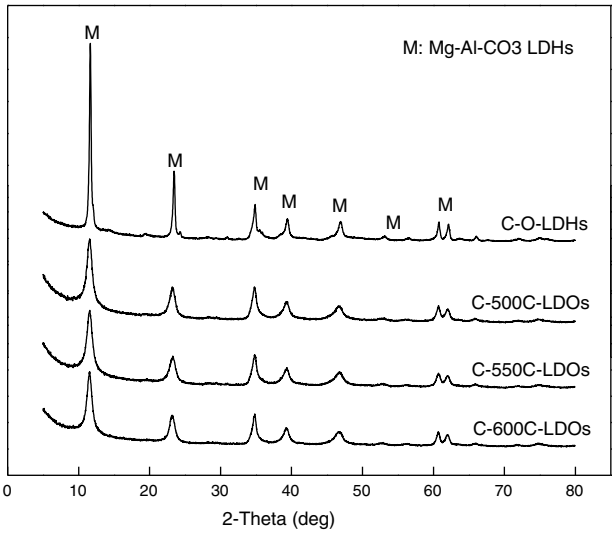

Fig. 2 – XRD patterns analyses of different types of LDHs.

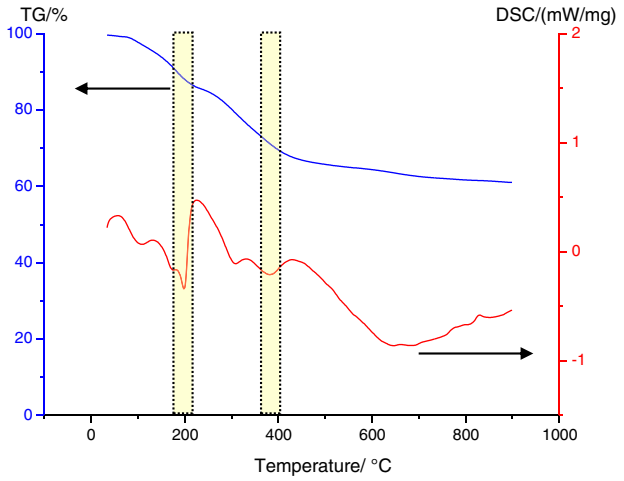

Fig. 3 – TG/DSC of Mg–Al–CO_3 type hydrotalcite.

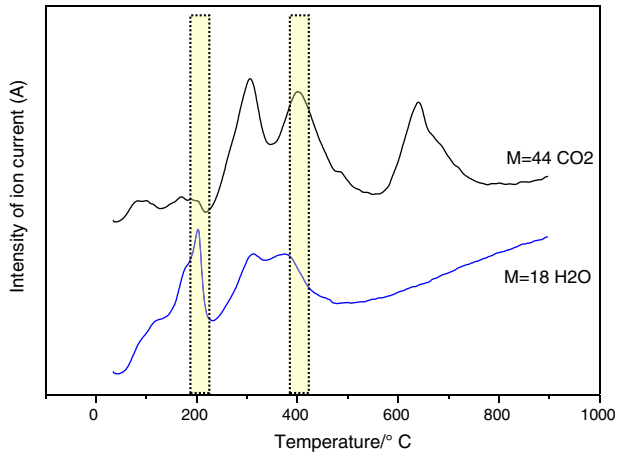

Fig. 4 – Mass spectrometry of Mg–Al–CO_3 type hydrotalcite.

respectively) display powder X-ray diffraction spectra typical of LDH materials (shown in Fig. 2). However, the broad peaks are presumably due to the simultaneous effects of small coherent domain size and structural disorder after calcinations at different temperature. The XRD patterns of LDHs indicate that the layer structure does not collapse with the loss of interlayer water.

3.2. *Thermal decomposition of hydrotalcite-like compounds*

According to the literature [17–19] the thermal decomposition of LDHs includes three main stages, i.e., the removal of interlayer water, the decomposition of structural hydroxyl groups and finally the decomposition of interlayer carbonate anions as shown in Figs. 3 and 4.

The results show an initial reduction in weight between RT and 200 °C arising from physical absorbed and interlayer water (see the first peak of H_2O in Fig. 4). A second weight loss between 200 and 400 °C results from a concomitant dehydroxylation of the layers and a reduction of CO_3^{2-} to CO_2 (see the second peak of H_2O and peaks of CO_2 in Fig. 4). A temperature treatment beyond 500 °C caused a collapse of

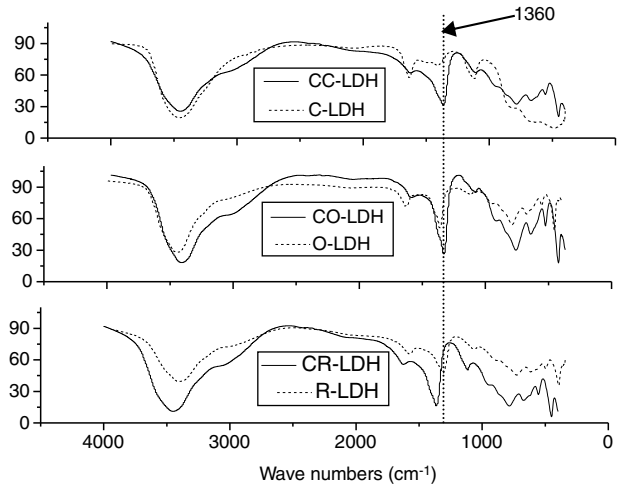

Fig. 5 – Infrared analysis of LDHs before and after CO_2 capture.

Table 3 – Wave numbers correspond to infrared absorption band of LDHs (cm^{-1}).

	O-LDH	C-LDH	R-LDH
Bending vibration of –OH	1637	1636	1637
Stretching vibration of –OH	3442	3454	3461
Stretching vibration of C–O	1360	1409	1364
Bending vibration of CO_3^{2-}	789–673	813	782–671

the layered structure for all compounds and gave rise to new crystalline phases due to the decomposition of interlayer carbonate anions (see the last peak of CO_2 in Fig. 4) (mixed oxides, e.g., spinel forms).

3.3. *Infrared analysis of LDHs before and after carbonation test*

The carbonation test was done inside a chamber with a CO_2 concentration ≈20% ± 3%, RH ≈ 70% ± 5%, and $T \approx 20\,^{\circ}C \pm 3\,^{\circ}C$. Different series of LDHs was mixed with water with constant ratio of 1:10, which were vigorously stirred. After that, the solutions were moved into the carbonation chamber for 24 h.

FTIR spectroscopy showed characteristics frequencies associated with the types of LDHs. Fig. 5 shows the FT-IR spectra of LDHs calcined at different temperature before and after CO_2 capture. Original LDHs before and after CO_2 capture hereafter were referred to as O-LDH and CO-LDH, respectively. LDHs calcined at 600 °C before and after CO_2 capture hereafter were referred to as C-LDH and CC-LDH, respectively. Calcinated LDHs mixing with water for structure regeneration before and after CO_2 capture hereafter were referred to as R-LDH and CR-LDH, respectively.

Table 3 summaries the wave numbers correspond to infrared absorption band of LDHs before and after CO_2 capture.

In Fig. 5 and Table 3, absorption band of stretching vibration of C–O, shift to higher wave number (from 1360 to 1409) in the process of O-LDH changes to C-LDH after calcination, and absorption band of stretching vibration of C–O, shift to lower wave number (from 1409 to 1364) in the construction regeneration process of C-LDH changes to R-LDH after mix with

water. Similar wave number corresponding to C–O, CO_3^{2-} of O-LDH and R-LDH indicates reconstruction of layered structure of LDHs.

In all the curves, the absorption band of the three types of LDHs before and after carbonation are similar, the intensity of absorption band of stretching vibration of C–O increases after carbonation, it shows the content of CO_3^{2-} in layered structure of LDHs increases after carbonation, especially for the C-LDH. The absorption band of O-LDH, CO-LDH, C-LDH, CC-LDH indicates that the intensity of bending vibration of –OH decreases after carbonation, some factors leading to this phenomenon can be summarized as following: (1) CO_2 changes to CO_3^{2-} when mixing with water molecular, and ion exchange occurs between CO_3^{2-} and OH^-, therefore, OH^- was substituted by CO_3^{2-}; (2) samples are mix with water before carbonation, water molecular enters into the layered structure and the increasing interlayer spacing is beneficial for intercalation and exchange of CO_3^{2-}; (3) acid gas CO_2 will lower the pH of cement paste.

3.4. *Impact of structure evolution on CO_2 sorption*

Evolution of the structure taking place during and after the thermal decomposition of the Mg–Al–CO_3 LDHs is very important for understanding its CO_2 sorption properties. In the crystalline phase, LDHs consists of positively charged Mg–Al–OH brucite type layers in an octahedral network. The surface and structural properties of LDHs in this phase are not suitable for reversible CO_2 sorption, as the Mg–OH-rich network in the crystalline LDHs has been found to favor base-catalyzed reactions. Hence, the sorption in this phase is mostly attributed to the acid–base reaction of Mg–OH and CO_2 forming $Mg(HCO_3)_2$, which is considered to be irreversible sorption.

On the other hand, LDHs completely loses interlayer water and dehydroxylates to a large extent upon heating to 600 °C, leading to the formation of a mixed oxide with a three dimensional network. Although a fair amount of carbonate still remains in the structure, this gives a relatively high surface area and exposes sufficient basic sites on the surface. These basic sites favor reversible CO_2 sorption in a form as follows

$$Mg–O + CO_2 = Mg–O\cdots CO_2(ad) \quad (1)$$

The interaction between the adsorbed CO_2 and the basic sites seems to be mainly responsible for CO_2 sorption at 600 °C. The experimental results obtained in our studies suggest that this interaction is not as weak as in the case of zeolite but not as strong as in the case of alkali metal oxide. These results strongly suggest the potential of LDOs use as a CO_2 sorbent in flue gas systems at temperatures around 600 °C and above.

However, the R-LDH accumulates significant mass during its aging period because of interactions with atmospheric water and CO_2. This led to the hydroxylation of metal oxides, particularly on the surface, with a partial revival of the crystalline LDHs structure in addition to the physical bonding of water. The same diffraction peaks of O-LDHs and R-LDHs by XRD analysis indicate reconstruction of C-LDHs after reaction with water. The XRD patterns of LDHs before and after calcinations indicate that the regeneration of layer structure of calcined LDHs, which leads to hydroxylation of mental oxides. The results of FTIR of LDHs and concrete before and after carbonation also confirm a successful intercalation of CO_3^{2-} in DLHs, which fulfills the structure regeneration, i.e., the revival of the crystalline LDHs structure [20].

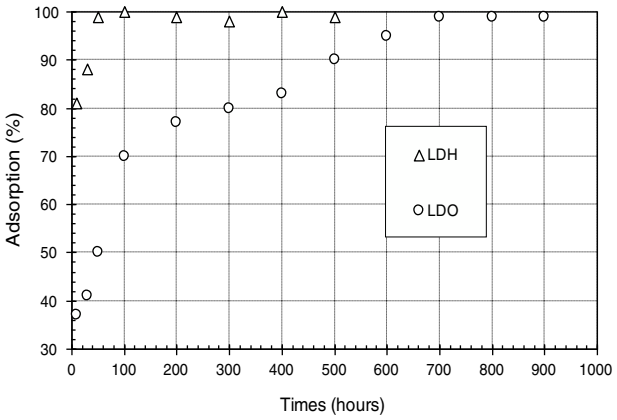

Fig. 6 – Time dependence of adsorption of CO_3^{2-} by LDHs and LDOs.

The partial reconstruction of the mixed oxide to the LDHs phase on the surface of the R-LDH sample thus decreases the CO_2 sorption capacity. As a consequence, recalcination of the R-LDH restores both the amorphous mixed oxide and CO_2 sorption capacity [20]. On account of these observations, either vacuum storage of the LDOs or in situ calcination methods were used for all further CO_2 sorption measurements. In the in situ calcination method, LDHs was calcined in conjunction with CO_2 sorption measurements. These methods produced highly consistent sorption values.

3.5. *Adsorption experiments*

Adsorption equilibrium for CO_3^{2-} by LDHs was achieved within 100 h, whereas more than 700 h were needed for calcined LDHs (LDOs) (Fig. 6). This indicates that the adsorption mechanism of CO_3^{2-} to LDH is different from that of LDO. Layered double hydroxide exhibits selectivity for the anions in the sequence $CO_3^{2-} > SO_4^{2-} > Cl^-$, therefore, ion exchange will not occur between CO_3^{2-} and untreated Mg–Al–CO_3 type LDHs, CO_3^{2-} was adsorbed on external surface of LDH. However, LDH calcined at 600 °C, namely, LDOs, provides large amounts of basic sites for CO_3^{2-} to occupy in the interlayers, therefore, adsorption mechanism of CO_3^{2-} to LDOs are structure regeneration through memory effect.

Additionally, larger sulfate anions with higher electric charge can intercalate easily between the layers to maintain electroneutrality or exchange other anions. Planar structure of CO_3^{2-} leads to the most stable structure forms only when it intercalates parallelly with the layer structure. Therefore, interlayer spacing decreases when CO_3^{2-} intercalates between the layers, basic sites for CO_3^{2-} are less and adsorption equilibrium for CO_3^{2-} in LDHs achieves within shorter time compared to LDOs.

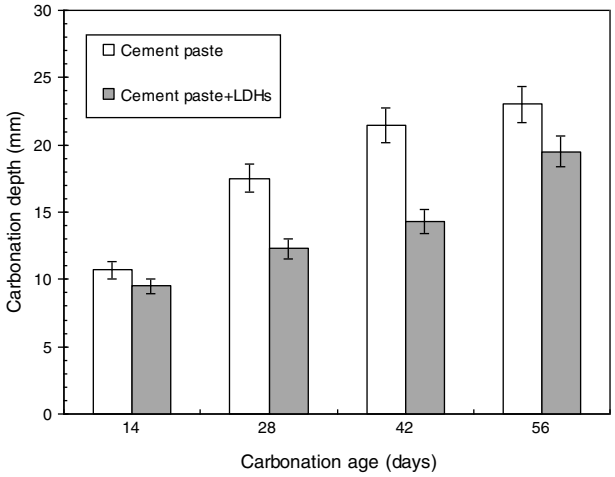

Fig. 7 – Carbonation depth of cement paste mixtures containing LDHs at different ages.

3.6. *Carbonation depth of cement paste*

The carbonation depth of cement paste mixtures containing LDHs is plotted as a function of carbonation ages in Fig. 7.

In Fig. 7, carbonation depth of all samples decreases with addition of calcined LDHs regardless of curing ages, however, the reduction at early ages (14 days) is negligible, carbonation depth results indicate that LDHs have positive effect on improvement of carbonation resistance of cement paste especially for sample at 42 days with the most dramatic reduction of carbonation depth, i.e., 30.8%. At 14 days, the effect of LDHs on the improvement of carbonation depth is not significant as later curing stages. However, after 28 days, carbonation depth of all samples decreases significantly when incorporating LDHs.

The results shown in Fig. 7 indicate that LDHs have positive effect on improvement of carbonation resistance of cement paste especially at later curing stages. Calcined LDHs will adsorb large amounts of CO_3^{2-} anions in layer with the change of CO_3^{2-} to CO_2 after calcinations, and the reconstruction after reaction with H_2O and CO_2 leads to consumption of large amounts of CO_2 in cement paste.

4. Conclusions

The component and structural changes of original LDHs, LDHs calcined at 500, 550 and 600 °C, respectively, before and after CO_2 capture, carbonation resistance of cement paste incorporating LDHs and ion exchange mechanism of LDHs from thermodynamic calculation were presented in this paper. From the results obtained in this study, the following conclusions can be drawn:

(1) LDH-like materials could be used in cement and concrete for their CO_3^{2-} capturing capacity and to enhance carbonation resistance of concrete as well as eliminate carbon dioxide's impact on climate change especially the LDHs calcined at 600 °C.

(2) All the solids including original LDHs, and LDHs calcined at 500, 550 and 600 °C, respectively, after CO_2 capture display powder X-ray diffraction spectra typical of LDHs materials. Broad peaks are presumably due to the simultaneous effects of small coherent domain size and structural disorder after calcinations at different temperature.

(3) Thermal decomposition of LDHs includes three main stages, i.e., the removal of interlayer water, the decomposition of structural hydroxyl groups and finally the decomposition of interlayer anions.

(4) The content of CO_3^{2-} in layered structure of LDHs increases after CO_2 capture. LDHs have positive effect on improvement of carbonation resistance of cement paste especially at later curing stages.

Conflicts of interest

The authors declare no conflicts of interest.

Acknowledgements

This work was financially supported by National Natural Science Foundation of China (No. 51508191 and No. 51502272), the Fundamental Research Funds for the Central Universities, China University of Geosciences (Wuhan) (No. G1323511668), the Foundation from State Key Laboratory of Silicates Materials for Architectures of Wuhan University of Technology (SYSJJ2014-3, SYSJJ2018-15), and the Opening Project of Engineering Research Center of Nano-Geo Materials of Ministry of Education, China University of Geosciences (NGM2018KF011).

REFERENCES

[1] Newman ACD. Chemistry of clays and clay minerals. New York: Wiley-Interscience; 1987.
[2] Cavani C, Trfiro E, Vaccari A. Hydrotalcite-type anionic clays: preparation, properties and applications. Catal Today 1991;11:173–201.
[3] Khan IA, Ohare D. Intercalation chemistry of layered double hydroxides: recent developments and applications. J Mater Chem 2002;12:3191–8.
[4] Taylor HFW. Cement chemistry. 2nd ed. London: Thomas Telford Publishing; 1997.
[5] Constantino VRL, Pinnavaia TJ. Basic properties of $Mg^{2+}_{1-x}Al^{3+}_x$ layered double hydroxides intercalated by carbonates, hydroxide, chloride, and sulfate anions. Inorg Chem 1995;34:883–92.
[6] Carlino S. The intercalation of carboxylic acids into layered double hydroxides: a critical evaluation and review of the different methods. Solid State Ionics 1997;98:73–84.
[7] Gardner EA, Sang KY, Kwon T, Pinnavaia TJ. Layered double hydroxides pillared by macropolyoxometalates. Appl Clay Sci 1998;13:479–94.
[8] Raki L, Rancourt DG, Detellier C. Preparation, characterization, and Mossbauer spectroscopy of organic anion intercalated pyroaurite-like layered double hydroxides. Chem Mater 1995;7:221–4.
[9] Beres A, Palinko I, Kiricsi I, Nagy JB, Kiyozumi Y, Mizukami F. Layered double hydroxides and their pillared derivatives-materials for solid base catalysis: synthesis and characterization. Appl Catal A: Gen 1999;182:237–47.

[10] Rives V, Ulibarri MA. Layered double hydroxides (LDH) intercalated with metal coordination compounds and oxometalates. Coord Chem Rev 1999;181:61–120.
[11] Alejandre A, Medina F, Slargre P, Correig X, Sueiras JE. Preparation and study of Cu–Al mixed oxides via hydrotalcite-like precursors. Chem Mater 1999;11:939–48.
[12] Pavan PC, Gomes G, Valim JB. Adsorption of sodium dodecyl sulfate on layered double hydroxides. Microporous Mesoporous Mater 1998;21:659–65.
[13] Choy JH, Kwak SY, Park JS, Jeong YJ, Portier J. Intercalative nanohybrids of nucleoside monophosphates and DNA in layered metal hydroxide. J Am Chem Soc 1999;121:1399–400.
[14] Whilton NT, Vickers PJ, Mann SJ. Bioinorganic clays: synthesis and characterization of amino- and polyamino acid intercalated layered double hydroxides. J Mater Chem 1997;7:1623–9.
[15] Caravaggio GA, Detellier C, Wronski Z. Synthesis, stability and electrochemical properties of NiAl and NiV layered double hydroxides. J Mater Chem 2001;11:912–21.
[16] Lotsch B, Millange F, Walton RI, Ohare D. Separation of nucleoside monophosphates using preferential anion exchange intercalation in layered double hydroxides. Solid State Sci 2001;3:883–6.
[17] Miyata S. Physicochemical properties of synthetic hydrotalcites in relation to composition. Clays Clay Miner 1980;28:50–6.
[18] Rives V. Characterisation of layered double hydroxides and their decomposition products. Mater Chem Phys 2002;75:19–25.
[19] Vagvolgyi V, Palmer SJ, Kristof J, Frost RL, Horvath E. Mechanism for hydrotalcite decomposition: a controlled rate thermal analysis study. J Colloid Interface Sci 2008;318:302–8.
[20] Duan P, Chen W, Ma JT, Shui ZH. Influence of layered double hydroxides on microstructure and carbonation resistance of sulphoaluminate cement concrete. Constr Build Mater 2013;48:601–9.